

# Na<sub>8</sub>[Cr<sub>4</sub>B<sub>12</sub>P<sub>8</sub>O<sub>44</sub>(OH)<sub>4</sub>][P<sub>2</sub>O<sub>7</sub>] $\cdot$ *n*H<sub>2</sub>O: A 3D Borophosphate Framework with Spherical Cages

Tao Yang,<sup>[a]</sup> Junliang Sun,<sup>[b]</sup> Guobao Li,<sup>[a]</sup> Lars Eriksson,<sup>[b]</sup> Xiaodong Zou,<sup>[b]</sup>  
Fuhui Liao,<sup>[a]</sup> and Jianhua Lin<sup>\*[a]</sup>

**Abstract:** A chromium borophosphate–phosphate (Na<sub>8</sub>[Cr<sub>4</sub>B<sub>12</sub>P<sub>8</sub>O<sub>44</sub>(OH)<sub>4</sub>][P<sub>2</sub>O<sub>7</sub>] $\cdot$ *n*H<sub>2</sub>O, **1**), which has an unusual 3D framework structure, was synthesized under hydrothermal conditions. The framework consists of spherical cages composed of CrO<sub>6</sub>, PO<sub>4</sub>, BO<sub>4</sub>, and BO<sub>3</sub> polyhedra. The cages are located at the vertices and the body center of the cubic cell and are interconnected through 12-membered-ring windows along the {111} direction. The

actual framework structure is very complex, but the description can be simplified by using the 5-connected fundamental building cluster [CrP<sub>5</sub>B<sub>3</sub>O<sub>24</sub>]<sup>11-</sup>. In addition, **1** represents the first borate-rich borophosphate that contains a 3D borophos-

phosphate partial framework ( $\infty^3$ -[B<sub>3</sub>P<sub>2</sub>O<sub>11</sub>(OH)]) in which the fundamental building unit is an oB dreier single ring ( $\Delta 4\Box:\Box < \Delta 2\Box > \Box$ ). The cavities of the framework are filled with disengaged water molecules and Na<sup>+</sup> counterions. The former can be reversibly desorbed and reabsorbed and the latter can be exchanged by Li<sup>+</sup> ions, which results in significant shrinkages of the cell volume.

**Keywords:** borophosphate • cage compounds • chromium • structure elucidation

## Introduction

Open-framework inorganic materials are of great interest due to their wide applications in sorption and separation, heterogeneous catalysis, and ion exchange.<sup>[1]</sup> In addition to the silicates, aluminosilicates, and aluminophosphates, the research on borophosphates has been growing<sup>[2]</sup> and a great number of new compounds have been reported in the last decade.<sup>[3]</sup> Because boron may adopt four- or three-fold coordination, the borophosphate frameworks are often more complicated than tetrahedral frameworks, although there are indeed a number of borophosphates known to adopt zeolite-type structures.<sup>[4–9]</sup> Despite the diverse structures, a

few principles and fundamental building units (FBUs) have been proposed by Kniep et al.,<sup>[10]</sup> which are useful to guide our understanding of borophosphate structures. For simplicity, they disregarded the polyhedra of metal atoms and mainly focused on the anionic partial structures of borophosphates. Thus, the framework structures of borophosphates known so far can be derived from a few typical borophosphate FBUs. This description reveals that most of the borophosphate partial structures are low dimensional, with only two exceptional 3D cases, M<sup>I</sup>[B<sub>2</sub>P<sub>2</sub>O<sub>8</sub>(OH)] (M<sup>I</sup>=Rb, Cs)<sup>[11]</sup> and A[BeBP<sub>2</sub>O<sub>8</sub>] $\cdot$ *n*H<sub>2</sub>O (A=Na<sup>+</sup>, K<sup>+</sup>, NH<sub>4</sub><sup>+</sup>).<sup>[7]</sup> Nevertheless, to describe the complete framework, one has to include the polyhedra of metal atoms, in particular, the octahedra and tetrahedra. A useful approach is to describe framework structures by using metal borophosphate clusters as building units. For example, [template] $\cdot$ [MB<sub>2</sub>P<sub>3</sub>O<sub>12</sub>(OH)] (M=Co,<sup>[12]</sup> Mn<sup>[13]</sup>) can be considered as a simple cubic porous framework built up with the six-connected building cluster [MP<sub>4</sub>B<sub>2</sub>O<sub>20</sub>]<sup>12-</sup>, as shown in Figure 1a. A similar building unit ([VP<sub>4</sub>B<sub>3</sub>O<sub>16</sub>(OH)<sub>5</sub>]<sup>4-</sup>) was found in [N<sub>2</sub>C<sub>6</sub>H<sub>14</sub>]<sub>2</sub>VO(PO<sub>3</sub>OH)<sub>4</sub>(B<sub>3</sub>O<sub>3</sub>OH) $\cdot$ 4H<sub>2</sub>O,<sup>[14]</sup> but with an additional BO<sub>3</sub> that forms a typical 3-membered borate ring (see Figure 1b). This is a similar approach to that used in so-called “scale chemistry”, in which large polynuclear clusters are used as building blocks to construct micro- or even mesoporous compounds.<sup>[15–18]</sup>

[a] T. Yang, Dr. G. Li, F. Liao, Prof. Dr. J. Lin  
Beijing National Laboratory for Molecular Sciences  
State Key Laboratory for Rare-Earth Materials Chemistry  
and Applications  
College of Chemistry and Molecular Engineering  
Peking University, Beijing, 100871 (China)  
Fax: (+86)10-6275-1708  
E-mail: jhlin@pku.edu.cn

[b] Dr. J. Sun, Dr. L. Eriksson, Prof. Dr. X. Zou  
Structural Chemistry, Stockholm University  
10691, Stockholm (Sweden)

Supporting information for this article is available on the WWW under <http://dx.doi.org/10.1002/chem.200800789>.

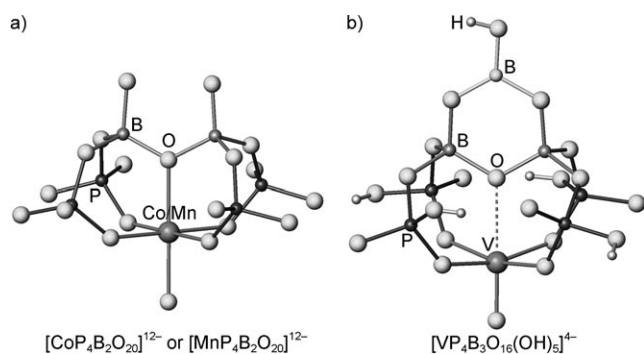


Figure 1. A schematic view of a)  $[\text{CoP}_4\text{B}_2\text{O}_{20}]^{12-}$  or  $[\text{MnP}_4\text{B}_2\text{O}_{20}]^{12-}$  and b)  $[\text{VP}_4\text{B}_3\text{O}_{16}(\text{OH})_5]^{4-}$ .

We report herein a new chromium borophosphate–phosphate,  $\text{Na}_8[\text{Cr}_4\text{B}_{12}\text{P}_8\text{O}_{44}(\text{OH})_4][\text{P}_2\text{O}_7] \cdot n\text{H}_2\text{O}$  (**1**) that contains  $\text{CrO}_6$  octahedra,  $\text{BO}_4$  and  $\text{PO}_4$  tetrahedra, and  $\text{BO}_3$  triangles. The complicated structure of **1** can be described as a cage framework with  $[\text{CrP}_5\text{B}_3\text{O}_{24}]^{11-}$  as the building unit. As we will show later, the  $[\text{CrP}_5\text{B}_3\text{O}_{24}]^{11-}$  cluster adopts a similar structure to that in Figure 1, but is a 5-connected unit and thus the topology of the cage framework is rather unusual. Additionally, **1** is also the first borate-rich example that contains a 3D borophosphate partial framework (see Scheme S1 in the Supporting Information). The resident metal cations in the cage can be exchanged, which causes a significant change in the unit cell constants.

## Results and Discussion

**Structure description:** The as-synthesized crystals are large and appear to have a well-defined cubic morphology. However, the collected X-ray diffraction data exhibited weak super-reflections, which indicates a deviation from the high-symmetry structure. Attempts to solve the structure accurately, such as collecting data on different crystals at low temperature by using a synchrotron X-ray source, carrying out the structure refinement by including the satellite reflections, or by using primary cubic symmetry, were all unsuccessful.<sup>[19]</sup> Therefore, we have described the average structure (the space group is  $I23$ ) based only on the main reflections. In fact, the average structure represents the structural feature of the frame-

work rather nicely. Unusually large anisotropic displacement factors have been observed mainly for the isolated  $\text{P}_2\text{O}_7$  group and some of the oxygen atoms, which have then been described by using the splitting model.

The structure of **1** consists of a porous framework of  $\{[\text{Cr}_4\text{B}_{12}\text{P}_8\text{O}_{48}][\text{P}_2\text{O}_7]\}^{12-}$ , counterions ( $\text{Na}^+$ ), and absorbed water. The framework is well defined and consists of 22 crystallographically independent atoms: 1 Cr, 15 O, 3 P, and 3 B.<sup>[20]</sup> All the atoms in the framework are located in general positions except for O14, which is located on the 2-fold axis (site 12d). To simplify the expression of the framework in **1**, one can define  $[\text{CrP}_5\text{B}_3\text{O}_{24}]^{11-}$  as the fundamental building cluster (see Figure 2a), in which the polyhedra are linked in a similar fashion to that observed in the cluster  $[\text{VP}_4\text{B}_3\text{O}_{16}(\text{OH})_5]^{4-}$ .<sup>[14]</sup> The central  $\text{CrO}_6$  octahedron is surrounded by 4 P1- and P2-centered  $\text{PO}_4$  tetrahedra in a square geometry by sharing corners that further connect to the  $\text{B}_3\text{O}_8$  borate ring. An additional P3-centered  $\text{PO}_4$  tetrahedron is present to complete the linkage of the  $\text{CrO}_6$  octahedron. In fact, the P3-centered tetrahedron is a part of a  $\text{P}_2\text{O}_7$  group in the structure, in which, as shown in Figure 2a and b, the O13 atoms are shared by neighboring  $\text{CrO}_6$  and the O15 atoms are terminal oxygen atoms. In the present average structure, the  $\text{P}_2\text{O}_7$  group is described by the splitting model with two orientations (related by 222-point symmetry). Although the present study does not provide the complete structure solution, it is a convincing possibility

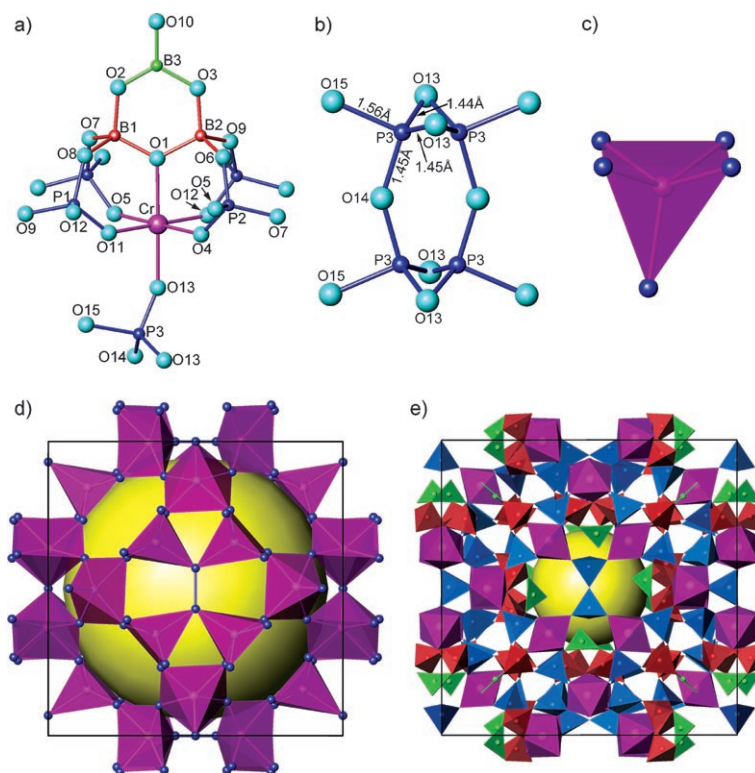


Figure 2. a) The building cluster  $[\text{CrP}_5\text{B}_3\text{O}_{24}]^{11-}$ , b) the two orientations of the  $\text{P}_2\text{O}_7$  group in the structure, c) the simplified square pyramidal unit (purple: Cr, deep blue: P), d) the topological linkage of the spherical cage expressed by square pyramids, and e) a projection of the structure of **1** along the  $\{001\}$  direction. Purple:  $\text{CrO}_6$ , blue:  $\text{PO}_4$ , red:  $\text{BO}_4$ , and green:  $\text{BO}_3$ . The large yellow spheres are present to guide the eye.

that the different orientations of the  $P_2O_7$  groups might be the major source of the super-reflections. The presence of the  $PO_4$  and  $P_2O_7$  groups in the structure was further confirmed by  $^{31}P$  magic-angle spinning (MAS) NMR spectroscopy (see Figure S1 in the Supporting Information). Two distinct resonance peaks were observed at about  $\delta = -5.8$  and  $-21.3$  ppm, which are attributed to the  $PO_4$  and  $P_2O_7$  groups, respectively, according to the literature.<sup>[21]</sup>

In the framework structure, the oxygen atoms on the P1- and P2-centered tetrahedra are further shared with the  $CrO_6$  and  $BO_4$  groups of the neighboring clusters, whereas the  $P_2O_7$  group connects four neighboring  $CrO_6$  octahedra. Thus the fundamental building cluster  $[CrP_3B_3O_{24}]^{11-}$  is actually 5-connected and can be simplified to a square pyramidal unit (see Figure 2c) in which only the Cr and P atoms are shown and the other atoms are omitted. Figure 2d shows a schematic view of the framework structure. It should be noted that the four basal  $PO_4$  groups are commonly shared by the neighboring square pyramidal units, whereas the axial  $PO_4$  groups are not only shared by two square pyramidal units, but are also interconnected to form the  $P_2O_7$  group (shown as a solid blue line). Therefore, **1** possesses an extended 3D cage framework structure, and the spherical cages are located at the vertices and the body center of the cubic cell. The actual framework structure is very complex (see Figure 2e) and consists of 24  $CrO_6$ , 60  $PO_4$ , and 24  $B_3O_8$  groups. The cavities of the cages are interconnected by 12- and 7-membered-ring windows composed, respectively, of 6  $PO_4$  and 6  $BO_4$  groups along the {111} direction and 4  $PO_4$  and 3  $CrO_6$  groups along the {001} direction. The Cr atoms in the framework structure are well separated by  $PO_4$  groups so that the magnetic susceptibility is predominantly paramagnetic with weak ferromagnetic interactions (see Figure S2 in the Supporting Information).

According to the structure analysis, the composition of the framework is  $\{[Cr_4B_{12}P_8O_{48}][P_2O_7]\}^{12-}$  ( $Z=6$ ). The negative charges of the framework are partially compensated by the protons bonded to the terminal oxygen atoms of the framework and partially by the  $Na^+$  cations in the cavity. The structure refinement reveals that some of the residual electron densities in the cavity can be assigned to the resident  $Na^+$  cations or  $H_2O$  molecules, whereas for those positions that are only partially occupied in the cavity, assignment is rather ambiguous due to similar scattering abilities and possible disorders. Alternatively, the amount of  $Na^+$  or  $H_2O$  present can be estimated from chemical analysis by inductively coupled plasma methods (ICP) and thermogravimetric analysis (TGA).

$Na^+$  quantities obtained for different as-synthesized samples by using ICP are listed in Table 1 and Table S1 in the Supporting Information. Although the data are dispersed, the mean value of the  $Na^+$  content is close to 2 (about 8  $Na^+$  ions per formula) for the as-synthesized samples. The TGA curve of as-synthesized **1** shows the two steps that give a total weight loss of 10.1 wt% (Figure 4). The first weight loss of 8.2 wt%, which occurs below 300 °C, should originate from the removal of the disengaged water molecules and

Table 1. Unit cell constants and atomic ratios of as-synthesized and treated samples.

Sample	<i>T</i> [h]	Atomic ratio (set P=2.50)					Volume [Å <sup>3</sup> ]	Volume ratio	
		Li+Na	Li	Na	Cr	B			P
<b>1</b>		2.21		2.21	0.99	3.15	2.50	8017(1)	1
<b>1</b> water-desorbed								7815(1)	0.9749
<b>1</b> water-re-absorbed								7961(1)	0.9930
<b>1</b> -Li-4	4	2.90	1.93	0.97	1.01	3.17	2.50	7516(2)	0.9375
<b>1</b> -Li-8	8	2.94	2.41	0.53	1.02	3.24	2.50	7358(3)	0.9178
<b>1</b> -Li-16	16	2.94	2.75	0.19	1.01	3.19	2.50	7300(3)	0.9106
<b>1</b> -Li-24	24	3.27	3.15	0.12	1.02	3.21	2.50	7256(4)	0.9051

the second weight loss of 1.9 wt% may originate from the dehydration of the hydroxyl groups. From the weight loss, one may estimate that there were about 8 disengaged water molecules (calcd: 7.95 wt% per formula) and 4 hydroxyl groups (calcd: 2.00 wt%). The presence of hydroxyl groups on the framework is also supported by the IR spectra (see Figure S3 in the Supporting Information). A sharp peak at  $\tilde{\nu} = 3590$   $cm^{-1}$  (assigned to the hydroxyl groups) that was observed in as-synthesized **1** disappears in deprotonated ( $Li^+$  exchanged) **1**. The other two bands at  $\tilde{\nu} = 3517$  and  $1629$   $cm^{-1}$ , which originate from  $H_2O$ , remain in both samples. From the structure, we know that there are two possible oxygen sites that may bond protons; one is the terminal oxygen (O10, general position) on  $BO_3$ , another is the terminal oxygen (O15, general position but half occupied) on the  $P_2O_7$  group. Considering the multiplicity factors of the two terminals and the acidity of boric and phosphoric acids, it seems more likely that the protons are bonded to the terminal oxygen on  $BO_3$ . Therefore, based on the structural and chemical analysis above and the charge balance, one can conclude that the overall composition of the as-synthesized **1** should be  $Na_8[Cr_4B_{12}P_8O_{45}(OH)_4][P_2O_7] \cdot 8H_2O$ .

**Borophosphate partial structure:** To further understand the structure, we have employed the Kniep's concept and nomenclature<sup>[10]</sup> of borophosphate FBUs to analyze the anionic partial structure of **1**. In Kniep's description, the transition metal can be ignored, thus one can focus mainly on the borophosphate partial structure. The  $P_2O_7$  group in **1** is an isolated phosphate group that can also be ignored. The FBU in **1** is, therefore, an oB dreier<sup>1</sup> single ring and can be expressed as  $\Delta 4 \square : \square < \Delta 2 \square > \square$  (Figure 3a; for an explanation of the descriptors and symbols, see ref. [10]). This borate-rich FBU has also been found in  $Na_2[M^{II}B_3P_2O_{11}(OH)] \cdot 0.67H_2O$  ( $M^{II} = Mg, Mn-Zn$ ).<sup>[22–24]</sup> The terminal oxygen atoms on both  $BO_4$  and  $PO_4$  are the atoms that could be shared by adjacent FBUs and in both **1** and  $Na_2[M^{II}B_3P_2O_{11}(OH)] \cdot 0.67H_2O$  the FBUs are 4-connected (exemplified in Figure 3b), which leaves two terminal

<sup>1</sup> The term "dreier" was coined by Liebau<sup>[30]</sup> and is derived from the German word drei, which means three.

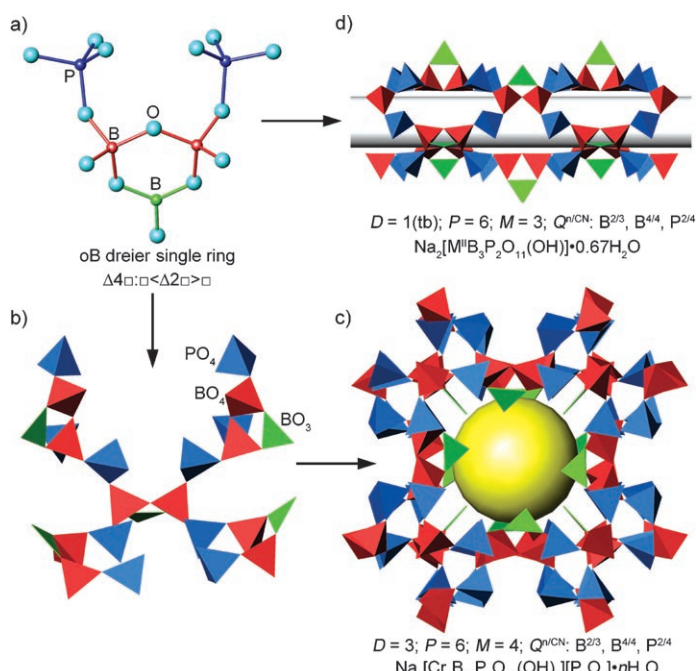


Figure 3. a) A single FBU of **1**, b) the connection between FBUs in **1**, c) the borophosphate partial structure in **1**, and d) the anionic partial structure in  $\text{Na}_2[\text{M}^{\text{I}}\text{B}_3\text{P}_2\text{O}_{11}(\text{OH})] \cdot 0.67\text{H}_2\text{O}$ . Blue:  $\text{PO}_4$ , red:  $\text{BO}_4$ , green:  $\text{BO}_3$ . The yellow sphere represents the spherical cage in the center.

oxygen atoms on  $\text{PO}_4$  coordinated to the transition metal cations. Although the local connections of the polyhedra are the same, the framework topologies are different in these two compounds, which is largely due to the flexible orientation of the  $\text{PO}_4$  group (for **1**:  $D = 3; P = 6; M = 4; Q^{n/\text{CN}}: \text{B}^{2/3}, \text{B}^{4/4}, \text{P}^{2/4}$  and for  $\text{Na}_2[\text{M}^{\text{I}}\text{B}_3\text{P}_2\text{O}_{11}(\text{OH})] \cdot 0.67\text{H}_2\text{O}$ :  $D = 1(\text{tb}); P = 6; M = 3; Q^{n/\text{CN}}: \text{B}^{2/3}, \text{B}^{4/4}, \text{P}^{2/4}$ ). As shown in Figure 3c, the borophosphate partial structure in **1** is a three dimensional framework consisting of spherical cages, which comprises a 3-connected topology with the Schläfli notation  $(6, 8^2, 12^2)_2^{[25]}$  (see Figure S4 in the Supporting Information). In  $\text{Na}_2[\text{M}^{\text{I}}\text{B}_3\text{P}_2\text{O}_{11}(\text{OH})] \cdot 0.67\text{H}_2\text{O}$ , however, the FBUs are interconnected in a parallel fashion that forms a tubelike 1D structure (see Figure 3d). It should be noted that, as far as we know, only two 3D borophosphate frameworks have been identified in the literature.  $\text{M}^{\text{I}}[\text{B}_2\text{P}_2\text{O}_8(\text{OH})]$  ( $\text{M}^{\text{I}} = \text{Rb}, \text{Cs}$ ) is a 1B dreier framework constructed by the fundamental building unit of  $4\Box:\Box<3\Box>\Box$ ,<sup>[11]</sup> whereas  $\text{A}[\text{BeBP}_2\text{O}_8] \cdot n\text{H}_2\text{O}$  ( $\text{A} = \text{Na}^+, \text{K}^+, \text{NH}_4^+$ ) is an oB achter framework composed of  $9\Box:\Box<6\Box>\Box|\Box|\Box$ .<sup>[7]</sup>

**Thermal stability and microporosity:** Figure 4 shows the TGA curves for **1** under different conditions. As-synthesized **1** exhibits two major weight losses. The first weight loss, which occurs below  $300^\circ\text{C}$ , mainly originates from the removal of the water molecules in the cavity and the second weight loss, which occurs between  $300$  and  $500^\circ\text{C}$ , is due to the dehydration of the hydroxyl groups. As shown in Figure 5, the powder X-ray diffraction patterns of a sample annealed at different temperatures (from  $25$  to  $800^\circ\text{C}$ ) indi-

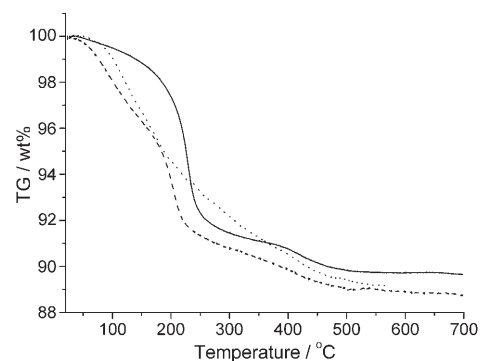


Figure 4. Thermogravimetric curves of as-synthesized **1** (—), water-reabsorbed **1** (----), and water-reabsorbed **1-Li-24** (.....).

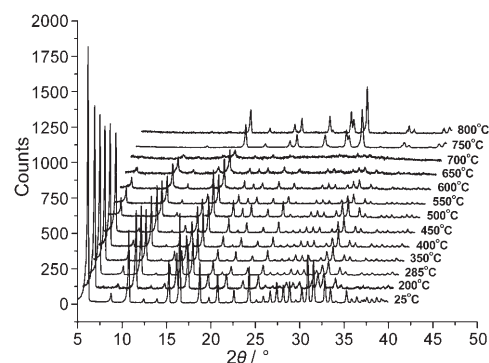


Figure 5. Powder X-ray diffraction patterns of as-synthesized **1** annealed at different temperatures ( $25$ – $800^\circ\text{C}$ ).

cates that the framework is retained until  $450^\circ\text{C}$ , above which the first reflection ( $110$ ) drops dramatically and the high  $2\theta$  reflections remain, which indicates that the framework collapses after the dehydration of the hydroxyl groups. At  $750^\circ\text{C}$ , a known condensed phase,  $\text{NaCrP}_2\text{O}_7$ , is formed.

The water molecules in the cavity of **1** can be reversibly desorbed and reabsorbed. To obtain a water-desorbed sample, we heated as-synthesized **1** at  $250^\circ\text{C}$  for 20 h. As shown in Figure 6, the X-ray diffraction pattern is almost identical to that of as-synthesized **1**, except for a slight

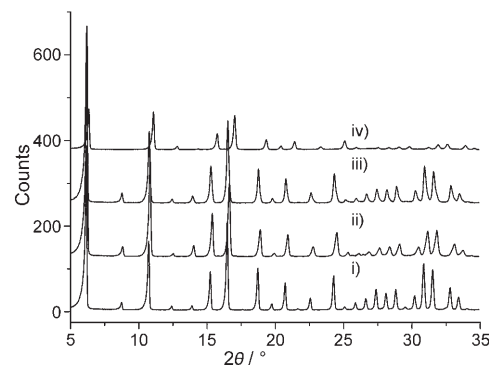


Figure 6. The powder X-ray diffraction patterns of i) as-synthesized **1**, ii) water-desorbed **1**, iii) water-reabsorbed **1**, and iv) **1-Li-24**.

shrinkage of the unit cell volume ( $\approx 2.5\%$ ). The cell volume can be completely restored by placing the desorbed sample in a water-saturated atmosphere for 20 h. The thermal behavior and crystalline integrity of water-reabsorbed **1** is similar to that of as-synthesized **1** (see Figure 4 and Figure 6).

The  $\text{Na}^+$  ions in the cavity of the framework are mobile and can be exchanged by  $\text{Li}^+$  ions. The exchange experiments were carried out by dipping as-synthesized **1** in molten  $\text{LiNO}_3$  at  $285^\circ\text{C}$ . After the exchange reaction, the products were extensively washed and sonicated several times with distilled water to ensure complete removal of the absorbed ions on the particle surface. The exchange reactions were carried out for periods of 4, 8, 16, and 24 h to give **1-Li-4**, **1-Li-8**, **1-Li-16**, and **1-Li-24**, and at each interval an ICP chemical analysis was performed and an X-ray diffraction pattern was recorded. It can be seen in Figure 6 that although the crystalline integrity of **1-Li-24** had declined, the framework was retained after a 24 h exchange reaction. In Table 1, we have summarized the results of chemical analysis and X-ray diffraction of the  $\text{Li}^+$ -exchanged samples. It can be seen that the  $\text{Li}^+$  content increases and the  $\text{Na}^+$  content decreases simultaneously over the course of the exchange reaction. At the same time, the unit-cell volume shrinks; for **1-Li-24**, the volume shrinkage is about 9.5%, which is significant for the exchange experiments. More interestingly, the overall cation contents ( $c(\text{Na}^+) + c(\text{Li}^+)$ ) in the  $\text{Li}^+$ -exchanged samples are all close to 3, an expected value for complete replacement of both  $\text{Na}^+$  ions and the protons of the hydroxyl groups (see Table 1). This implies that the  $\text{Li}^+$  ions preferentially replace the hydrogen atoms of the hydroxyl groups on the framework and then the  $\text{Na}^+$  ions in the cavity. The  $\text{Li}^+$  exchange was also verified by IR spectra and  $^7\text{Li}$  MAS NMR spectroscopy. As indicated, the sharp IR peak observed in the as-synthesized sample at  $\tilde{\nu} = 3590\text{ cm}^{-1}$  disappears in **1-Li-24**, which also exhibits two resonance signals centered at about  $\delta = -2$  and 29 ppm under the spectral frequency of 116.6 MHz and the magic-angle spinning speed of 13 kHz (see Figure S5 in the Supporting Information). Although we cannot absolutely assign the coordination environments of the two signals, the significantly different magnitudes suggest that the  $\delta = 29$  ppm signal may correspond to the  $\text{Li}^+$  ions that replace protons, whereas the  $\delta = -2$  ppm signal may correspond to the  $\text{Li}^+$  ions in the cavity. Additionally, **1-Li-24** reabsorbed in a water-saturated atmosphere also shows different thermal behavior (see Figure 4); it exhibits continuous weight loss without a plateau. All the above observations suggest that the replacement of  $\text{Li}^+$  with  $\text{H}^+$  does occur. We would like to point out that similar replacement has also been observed in other systems. For example,  $\text{H}_2\text{M}_2\text{PO}_7$  ( $\text{M} = \text{Ni}, \text{Co}$ )<sup>[26]</sup> is a hydrated metal phosphate; its lithium derivate  $\text{LiH}_3\text{M}_2(\text{P}_2\text{O}_7)_2$ ,<sup>[27]</sup> in which  $1/4$  of the protons on hydroxyl groups are replaced by  $\text{Li}^+$ , can be obtained by adding  $\text{LiNO}_3$  to the reaction systems.

The microporosity of **1** is exemplified by the reversibility of the water desorption/reabsorption and ion-exchange properties. In addition, the structure investigation definitely

shows that the large spherical cages are interconnected by 12-membered-ring windows. However, the BET surface area ( $N_2$ ) of **1** is rather small at about  $5\text{ m}^2\text{g}^{-1}$  (see Figure S6 in the Supporting Information), which means that **1** is not a traditional microporous material. Such a phenomenon is not uncommon and has been observed in other systems, such as  $\text{MCuB}_7\text{O}_{12}\cdot\text{H}_2\text{O}$  ( $\text{M} = \text{Na}, \text{K}$ ) in which the structure contains large 14-membered-ring channels.<sup>[28]</sup> We do not know the exact reason for this observation, but blocking of the windows by counterions, the hydrophilic nature of the inner surface, or even inappropriate experimental conditions may all result in such an observation. Nevertheless, the reversible water adsorption and ion-exchange properties verify that the guest species are mobile and that their mobility does not damage the integrity of the framework.

## Conclusion

$\text{Na}_8[\text{Cr}_4\text{B}_{12}\text{P}_8\text{O}_{45}(\text{OH})_4][\text{P}_2\text{O}_7]\cdot n\text{H}_2\text{O}$  is an interesting borophosphate-phosphate that adopts a spherical cage framework structure composed of  $\text{CrO}_6$ ,  $\text{PO}_4$ ,  $\text{BO}_4$ , and  $\text{BO}_3$  polyhedra. The cages are located at the vertices and the body center of the cubic cell and are interconnected through 12-membered-ring windows along the  $\{111\}$  direction. The desorption and absorption of the disengaged water molecules in the cavity are reversible. The  $\text{Na}^+$  counterions are exchangeable with  $\text{Li}^+$  ions, and this is accompanied with significant shrinkages of the unit cell. During the  $\text{Li}^+$ -exchange process, the framework is retained but the crystallization decreases. It is likely that the  $\text{Li}^+$  replaces not only the  $\text{Na}^+$  ions but also the hydrogen atoms on the framework. Additionally, the analysis based on Kniep's concept reveals that **1** adopts a 3D borophosphate partial framework structure, represented as  ${}_\infty^3[\text{B}_3\text{P}_2\text{O}_{11}(\text{OH})]$ . The FBU is an oB dreier single ring ( $\Delta 4\text{□} < \Delta 2\text{□} > \text{□}$ ). Interestingly, although another known borophosphate,  $\text{Na}_2[\text{M}^{\text{II}}\text{B}_3\text{P}_2\text{O}_{11}(\text{OH})]\cdot 0.67\text{H}_2\text{O}$  ( $\text{M}^{\text{II}} = \text{Mg}, \text{Mn-Zn}$ ), is also built up with a similar FBU, its framework structure is 1D and tubelike. As far as the structural chemistry of borophosphates is concerned and to the best of our knowledge, **1** represents the first borate-rich phase that contains a 3D borophosphate partial framework.

## Experimental Section

**Synthesis:** **1** can be synthesized by a hydrothermal reaction method. Typically,  $\text{Cr}(\text{NO}_3)_3\cdot 9\text{H}_2\text{O}$  (1.0 g, 2.5 mmol) was dissolved in concentrated  $\text{H}_3\text{PO}_4$  (3 mL,  $14.6\text{ mol L}^{-1}$ ) in a 50 mL Teflon reactor at  $80^\circ\text{C}$ . Then  $\text{Na}_2\text{B}_4\text{O}_7\cdot 10\text{H}_2\text{O}$  (3.8 g, 10 mmol) was added and the Teflon reactor was sealed in a stainless steel container. After heating at  $220^\circ\text{C}$  for 4 days and cooling to RT in 12 h, the solid sample was washed extensively with hot water ( $80^\circ\text{C}$ ) until the soluble components were completely removed. Dark green single crystals with a truncated cubic appearance were obtained in a yield of about 90% with respect to Cr. The reaction temperature and time are not constant and can vary from  $180$  to  $240^\circ\text{C}$  and from 3 d to 2 weeks.

**Analyses:** The chemical analyses were carried out by ICP methods by using an ESCALAB2000 analyzer. The TGAs were performed on a

Dupont 951 thermogravimetric analyzer in air with a heating rate of  $10^{\circ}\text{Cmin}^{-1}$  from 30 to  $800^{\circ}\text{C}$ . Powder X-ray diffraction data were collected at room temperature on a Rigaku D/Max-2000 with Cu  $K_{\alpha}$  radiation ( $\lambda = 1.5406 \text{ \AA}$ ) from a rotating anode. The tube voltage and current were 40 kV and 100 mA, respectively. The magnetic property of **1** was investigated with a Quantum Design MPMS-SS superconducting quantum interference device (SQUID) magnetometer at a temperature range of 2 to 300 K at 0.1 T. The isothermal magnetization curve was measured at 2 K up to an applied field of 7 T.

**Structure determination:** Single-crystal X-ray diffraction was performed at room temperature by using an Xcalibur diffractometer equipped with a CCD detector. The structure was solved by direct methods in the space group  $I23$  and refined by full-matrix least squares techniques against  $F^2$  by using the SHELX programs.<sup>[29]</sup> The data analysis reveals that the structure, in fact, deviates from the  $I$ -centered lattice. However, the additional reflections are extremely weak, even for the data collected at 100 K. In the  $I23$  structural model, the  $\text{P}(3)_2\text{O}_7$  groups are described as two different orientated species (see Figure 2b). A total of 118454 reflections, of which 4103 are unique, were collected in the region  $3.7^{\circ} < \theta < 34.5^{\circ}$  ( $\lambda = 0.71073 \text{ \AA}$ ).  $R_{\text{int}} = 0.0345$ ,  $R_1 = 0.0574$ , and  $wR_2 = 0.1536$  for all reflections. Crystal data and details of the structure determination are given in Table 2. The refined atomic parameters are given in Table S2 in the Supporting Information. Further details of the crystal structure investigation can be obtained from the Fachinformationszentrum Karlsruhe, 76344 Eggenstein-Leopoldshafen, Germany (fax: (+49)7247-808-666; e-mail: crysdata@fiz-karlsruhe.de) on quoting the depository numbers CSD-415997.

Table 2. The crystallographic parameters and refinement results of **1**.

	$\text{Na}_8\text{H}_{20}\text{Cr}_4\text{B}_{12}\text{P}_{10}\text{O}_{63}$
$M_r$	1859.50
$T$ [K]	290
$\lambda$ [ $\text{\AA}$ ]	0.71073
crystal size [mm]	$0.1586 \times 0.1644 \times 0.2285$
morphology	green, truncated cubic
space group	$I23$
$a$ [ $\text{\AA}$ ]	20.0242(3)
$V$ [ $\text{\AA}^3$ ]	8029.1(2)
$Z$	6
$\rho_{\text{calcd}}$ [ $\text{g cm}^{-3}$ ]	2.31
$\mu(\text{Mo } K_{\alpha})$ [ $\text{mm}^{-1}$ ]	1.295
coll. reflns	118454
indep. reflns	4103
$I > 2\sigma(I)$	4103
$\theta$ range [ $^{\circ}$ ]	3.7–34.5
GOF	1.008
$R_1[I > 2\sigma(I)]$	0.0574
$wR_2(\text{all data})$	0.1536

## Acknowledgement

We thank Prof. C. X. Guo for helpful discussions regarding the MAS NMR spectra. This work was supported by the National Nature Science Foundation of China.

- [1] A. K. Cheetham, G. Férey, T. Loiseau, *Angew. Chem.* **1999**, *111*, 3466–3492; *Angew. Chem. Int. Ed.* **1999**, *38*, 3268–3292.  
 [2] R. Kniep, G. Gözel, B. Eisenmann, C. Röhr, M. Asbrand, M. Kizilyalli, *Angew. Chem.* **1994**, *106*, 791–793; *Angew. Chem. Int. Ed. Engl.* **1994**, *33*, 749–751.

- [3] R. Kniep, H. Engelhardt, C. Hauf, *Chem. Mater.* **1998**, *10*, 2930–2934.  
 [4] R. Kniep, G. Schäfer, H. Engelhardt, I. Boy, *Angew. Chem.* **1999**, *111*, 3857–3861; *Angew. Chem. Int. Ed.* **1999**, *38*, 3641–3644.  
 [5] R. Kniep, G. Schäfer, H. Borrmann, *Z. Kristallogr. New Cryst. Struct.* **2000**, *215*, 335–336.  
 [6] I. Boy, F. Stowasser, G. Schäfer, R. Kniep, *Chem. Eur. J.* **2001**, *7*, 834–839.  
 [7] H. Y. Zhang, Z. X. Chen, L. H. Weng, Y. M. Zhou, D. Y. Zhao, *Microporous Mesoporous Mater.* **2003**, *57*, 309–316.  
 [8] M. Yang, J. H. Yu, P. Chen, J. Y. Li, Q. R. Fang, R. R. Xu, *Microporous Mesoporous Mater.* **2005**, *87*, 124–132.  
 [9] Y. X. Huang, Y. Prots, R. Kniep, *Chem. Eur. J.* **2007**, *13*, 1737–1745.  
 [10] B. Ewald, Y. X. Huang, R. Kniep, *Z. Anorg. Allg. Chem.* **2007**, *633*, 1517–1540.  
 [11] C. Hauf, R. Kniep, *Z. Naturforsch.* **1997**, *B52*, 1432–1435.  
 [12] S. C. Sevov, *Angew. Chem.* **1996**, *108*, 2814–2816; *Angew. Chem. Int. Ed. Engl.* **1996**, *35*, 2630–2632.  
 [13] Y. X. Huang, O. Hochrein, D. Zahn, Y. Prots, H. Borrmann, R. Kniep, *Chem. Eur. J.* **2007**, *14*, 1737–1745.  
 [14] R. P. Bontchev, J. Do, A. J. Jacobson, *Inorg. Chem.* **1999**, *38*, 2231–2233.  
 [15] G. Férey, C. Serre, C. Mellot-Draznieks, F. Millange, S. Surblé, J. Dutour, I. Margiolaki, *Angew. Chem.* **2004**, *116*, 6456–6461; *Angew. Chem. Int. Ed.* **2004**, *43*, 6296–6301.  
 [16] A. C. Sudik, A. P. Côté, A. G. Wong-Foy, M. O’Keeffe, O. M. Yaghi, *Angew. Chem.* **2006**, *118*, 2590–2595; *Angew. Chem. Int. Ed.* **2006**, *45*, 2528–2533.  
 [17] C. Livage, N. Guillou, J. Chaigneau, P. Rabu, M. Drillon, G. Férey, *Angew. Chem.* **2005**, *117*, 6646–6649; *Angew. Chem. Int. Ed.* **2005**, *44*, 6488–6491.  
 [18] R. Q. Zou, H. Sakurai, Q. Xu, *Angew. Chem.* **2006**, *118*, 2604–2608; *Angew. Chem. Int. Ed.* **2006**, *45*, 2542–2546.  
 [19] The low temperature synchrotron data (100 K) was collected at MAX-lab, Lund University, Sweden. The beamline is 1911-5 with a wavelength of 0.91  $\text{\AA}$ . We tried the space groups  $P23$  and  $R3$ , and both were unsuccessful.  
 [20] It should be noted that 6 oxygen atoms in the framework are refined as disordered atoms and split into two close and equivalent positions. For the convenience of the structure description, we treat them as a single atom by averaging the coordinates of two equivalent atoms.  
 [21] E. Pichot, J. Emery, M. Quarton, N. Dacheux, V. Brandel, M. Genet, *Mater. Res. Bull.* **2001**, *36*, 1347–1359.  
 [22] T. Yang, G. B. Li, J. Ju, F. H. Liao, M. Xiong, J. H. Lin, *J. Solid State Chem.* **2006**, *179*, 2534–2540.  
 [23] W. Liu, Y. X. Huang, R. Cardoso, W. Schnelle, R. Kniep, *Z. Anorg. Allg. Chem.* **2006**, *632*, 2143.  
 [24] M. Yang, J. H. Yu, J. C. Di, J. Y. Li, P. Chen, Q. R. Fang, Y. Chen, R. R. Xu, *Inorg. Chem.* **2006**, *45*, 3588–3593.  
 [25] E. Koch, W. Fischer, *Z. Kristallogr.* **1995**, *210*, 407–414.  
 [26] T. Yang, J. Ju, G. Li, S. Yang, J. Sun, F. Liao, J. Lin, J. Sasaki, N. Toyota, *Inorg. Chem.* **2007**, *46*, 2342–2344.  
 [27] T. Yang, S. Yang, F. Liao, J. Lin, *J. Solid State Chem.* **2008**, *181*, 1347–1353.  
 [28] T. Yang, G. Li, L. You, J. Ju, F. Liao, J. Lin, *Chem. Commun.* **2005**, *33*, 4225–4227.  
 [29] G. M. Sheldrick, SHELXS-97, Program for the solution of crystal structures, University of Göttingen, Göttingen, Germany, **1997**; SHELXL-97, Program for the refinement of crystal structures, University of Göttingen, Göttingen, Germany, **1997**.  
 [30] F. Liebau, *Structural Chemistry of Silicates*, Springer, Berlin, **1985**.

Received: April 25, 2008  
 Published online: July 15, 2008